TRACE IMPURITY EFFECT ON THE PRECIPITATION BEHAVIOUR OF COMMERCIALLY PURE ALUMINIUM THROUGH REPEATED MELTING

Mohammad Salim KAISER

Directorate of Advisory, Extension and Research Services
Bangladesh University of Engineering and Technology, Dhaka-1000, Bangladesh

Abstract

Precipitation behaviour of commercially available pure aluminium with trace impurities throughout repeated melting has been carried out. Cold rolled alloy samples are isochronally aged for 60 minutes at different temperatures. Isothermal ageing is carried out at 250°C temperatures of cold rolled samples for different time up to 240 minutes. Hardness values of the aged alloys have been measured to comprehend the precipitation behaviour of the alloys with trace impurities. Trace impurities causes small age hardening effect as well as they pin moving grain boundaries and inhibit grain growth. The kinetics of precipitation of metastable phase in trace added alloys are found to be controlled by the diffusion of GP zones in aluminium. The results of this study confirmed a positive influence of alloy remelting upon the material properties and structure. The SEM images of fracture surfaces show spherical "dimples" correspond to microvoids that initiate crack formation and with the increasing of impurities the dimples of the fracture surfaces ever more decrease and become shallower.

Keywords*: Aluminium, trace addition, precipitation behaviour, resistivity, microstructure.*

Introduction

Commercially pure aluminium contains minimum amount of impurities, normally bellow than 1wt%. It is extracted through the electrolytic cell process. Pure aluminium is very soft and ductile but has a high corrosion resistant and electrical conductivity properties [1, 2]. It is widely used for foil and conductor cables, but the application of Al expands to other fields by addition of small amount of other elements, thus forming alloys [3]. Different mechanical properties of Al alloy can be achieved as well as improved through the addition of different elements which statisfy the specific requirements [4-9]. Alloying elements may be classified as major elements, minor elements, microstructure modifier elements and impurity elements [10]. Major elements like Si, Cu, Mg etc. provide substantial strengthening and improvement of the work-hardening properties of aluminium. Minor elements for example Ni and Sn improve the hot hardness of the alloys. Microstructure modifier elements as Ti, B, Sr, Be, Mn, Cr etc. additions to aluminum alloys can strongly influence the precipitation process, including modifying the dispersion, morphology and crystal structure of the resulting precipitations. Impurity elements Fe and Zn improve the hardness of the al alloys [11-14].

Precipitates play a great role on the softening behaviour of the aluminium alloys. Small precipitates interact with the moving grain boundaries with a retarding pressure called the Zener drag [15]. The recovery, recrystallization and grain growth processes are normally unhurried by precipitates. The recrystallization may be stagnated under several situation as the high amount of precipitates present in to the alloys and the restoration of the microstructure

Corresponding author: mskaiser@iat.buet.ac.bd

occurs by extended recovery. In this case, the subgrain structure grows and the kinetics are controlled by the coarsening of the particles [16-18]. This is why studying the precipitation behaviour is important.

Solid impurities may be added into aluminum from different sources. During casting of aluminium the inclusions may come from the refractory linings of furnaces, ladles, reactors or launders and the melting environment. Thus the aim of this work is to assess the repeated melting influence upon the precipitation behaviour, thermomechanical properties and structure changes of the commercially pure aluminium.

Experimental

Alloys were prepared by casting in a natural gas-fired pit furnace. Preparation of these alloys the commercially pure aluminium ingot (99.80% purity) was taken as the starting material Alloy 1. Generally it belongs to 1100-series alloy. First the commercially pure aluminium was melted in a clay-graphite crucible idiom as Alloy 2 and then it is remelt again for preparing Alloy 3. During melting degasser, borax etc. is used as flux cover. An electronic controller was used to monitor the final temperature of the melt and tried to maintain the temperature around 780±15°C. Casting was done into a permanent mild steel metal mould to make bars of 17.0 x 51.0 x 200.0 mm in size. The metal mould was preheated at 250°C before pouring the materials. The experimental alloys were homogenized at a temperature of 450°C for 12 hours to redistribute the precipitating elements evenly through the part. The solid solution treatments were carried out at 525°C for two hours followed by quenching in water to get a super saturated single phase region. The chemical compositions of the alloys are listed in Table 1. Capacity of 10HP laboratory scale rolling mill was used for cold rolling of the homogenized and solution treated alloys.

Table 1. Chemical Composition of the Experimental Alloys (wt%)

Alloy	Si	Fe	Mg	Cu	Mn	Cr	Zn	Ni	Pb	Sn	Al
1	0.0210	0.1806	0.0016	0.0022	0.0021	0.0016	0.0004	0.0000	0.0000	0.0000	Bal
2	0.4647	0.5820	0.0071	0.0091	0.0041	0.0294	0.0553	0.0175	0.0065	0.0017	Bal
3	0.8357	0.6273	0.0061	0.0150	0.0185	0.0453	0.0526	0.0195	0.0085	0.0019	Bal

The samples for the cold rolling were prepared by machining in size of 16 x 16 x 50 mm and the deformation per pass was given about 1.0 mm. After cold rolling the samples were subjected to isochronal ageing at different temperature up to 400°C for one hour and isothermally at 250°C for different ageing times up to 240. Hardness of the different heat treated alloys processed with different time and temperatures was measured in Micro vickers hardness testing machine for assessing the age hardening effect of the alloys. Load of 1Kg and 10 seconds dwell time was applied for the Knoof indentor. Electrical conductivity of the different processed alloys was measured with the help of Electric Conductivity Meter, type 979. For this electrical conductivity measurement finished surface of 15 mm x 15 mm was prepared for all the samples through grinding and polishing. Then the conductivity data were converted to electric resistivity. Instron testing machine was used for tensile test at room temperature. The cross head speed of the machine was 1.5mm/m to maintain the strain rate of $10^{-3}s^{-1}$. The samples for this tensile test was prepared according to ASTM specification. The microstructure observations of all these samples were carried out using professional inverted metallurgical microscope. The heat-treated samples were polished sequentially with 2000 grade grinding paper and finally with alumina. For this study the polished samples were etched using Keller's reagent. A scanning electron micrographic (SEM) study was carried out using a JEOL scanning electron microscope with X-ray analyzer. XRD analysis of the heat treated samples was done to verify the different elements present in the

experimental alloys. Differential scanning calorimetry (DSC) studies were carried out with selected samples in a Du Pont 900 instruments. The weight of each chunk samples for DSC studies was about of 30 mg. The samples were equilibrated at 50ºC temperature, and heated over a temperature to 550ºC with preset heating rate of 10°C/min under N_2 gas atmosphere.

Results and Discussion

Cold rolling behaviour

Figure 1 shows the variation of hardness and electrical resistivity of commercially pure aluminium Alloy 1, trace added Alloy 2 and Alloy 3 with the percentages of cold deformation. The hardness of the alloys increases with scale of deformation owing to strain hardening (Fig. 1a). The increases of rolling reduction means more plastically deformed of the metal, as a result additional dislocations density are generated. The supplementary dislocations inside a material makes more strengthening of the material. Higher hardness values were obtained for trace added alloys than that of pure aluminium because the presence of different hard intermetallics of Si, Fe etc. It can be seen from the figure that the electrical resistivity slowly decreases with degree of deformation (Fig. 1b). The decrease in porosity of the alloy samples during cold rolling results in a decrease in the electrical resistivity. At higher deformation the resistivity increases due of material defect as dislocation density. The electron scattering into the material increases with the scale of cold-working. It is ascribed to the lattice distortion or internal fault of structure. Also, it shows that the electrical resistivity of pure aluminium is lower than trace added alloys, because the presence of second elements into the alloy always decreases the electrical conductivity of the alloy. Si and Fe have the notable influence on the increased electrical resistivity of pure Al [19-22].
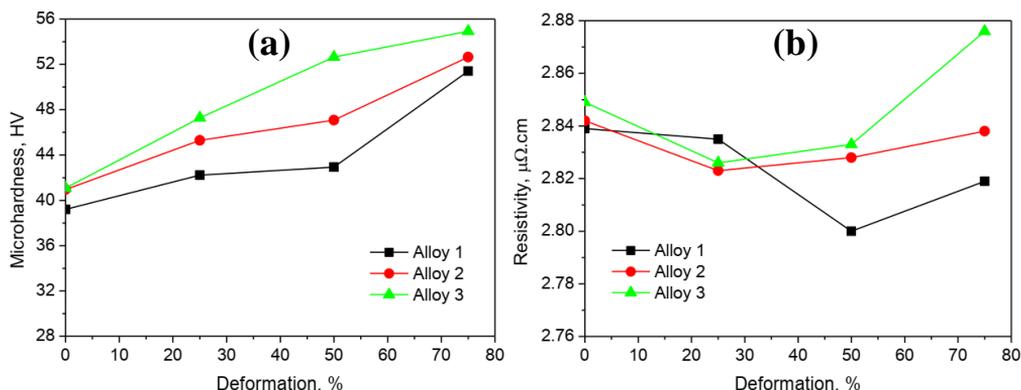

Fig. 1. Dependence of (a) hardness and (b) electrical resistivity of the alloys on degree of deformation

Age-hardening behaviour of cold-rolled alloys

The results of isochronal ageing of the cold worked alloys at different temperature for 1 hour are shown in Fig. 2. An initial softening is noted in almost all the alloys (Fig. 2a). The softening of the cold worked alloys at the initial stage of ageing is thought due to recovery as well as rearrangement of dislocations into the alloys [23]. It is seen that Alloy 1 shows a continuous softening but trace added Alloy 2 and Alloy 3 show small age hardening effect due to formation of GP zones and to metastable phases as they content impurities like Si, Cu, Ni, Mg etc. [24, 25]. Small variation of hardness into the peak is observed for dissolution of the GP-zones. However Alloy 3 shows the maximum hardness due to presence of higher intermetalics. When the alloys are aged at higher ageing temperatures beyond 250°C an

appreciable drop in hardness is observed for all the alloys due to precipitation coarsening and recrystallisation of the alloys. From the resistivity curve it is seen that all the alloys show a peak following an initial drop of resistivity (Fig. 2b). At low temperature drop of resistivity are responsible for thermally activated dislocation glide, recovery by annihilation and rearrangement of dislocations. In all the alloys resistivity peak are shown due to formation of GP zones as well as metastable phases. At higher temperature decreases of resistivity are liable for grain coarsening and recrystallization [26].
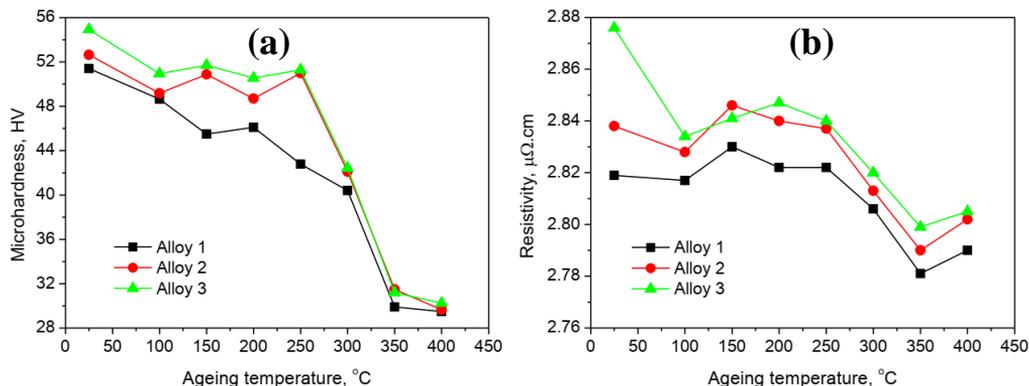

Fig. 2. Variation of (a) hardness and
(b) electrical resistivity of 75% cold rolled alloys with ageing temperature for one hour

The variations of the hardness and the electrical resistivity of the experimental alloys against isothermal aging at 250°C are shown in Fig. 3. At initial stage lower rate of softening be evidence for trace added Alloy 2 and Alloy 3. Commercially pure Alloy 1 shows an extremely quick and sharp decrease in hardness and get behind a constant value. Trace elements already presence into the alloys formed different intermetallic precipitates and those hinder the dislocation movement as a result limit the softening of the alloys (Fig. 3.a). In case of resistivity under same ageing condition the alloys shows an initial drop followed by increasing of resistivity and finally attain a slow but steady decrease (Fig. 3.b). Dislocation rearrangement takes place within the cold worked alloys during isothermal ageing which causes the initial drop in resistivity. The decrease in resistivity is found to be lower in Alloy 1 than all other trace added alloys. The rise in resistivity in all the alloys is due to the formation of G P zones and β'-metastable phase into the alloys. Finally a slow but steady decrease in resistivity occurs because of particle coarsening becomes as prominent as to diminish the incoherent scattering of electron [27, 28].
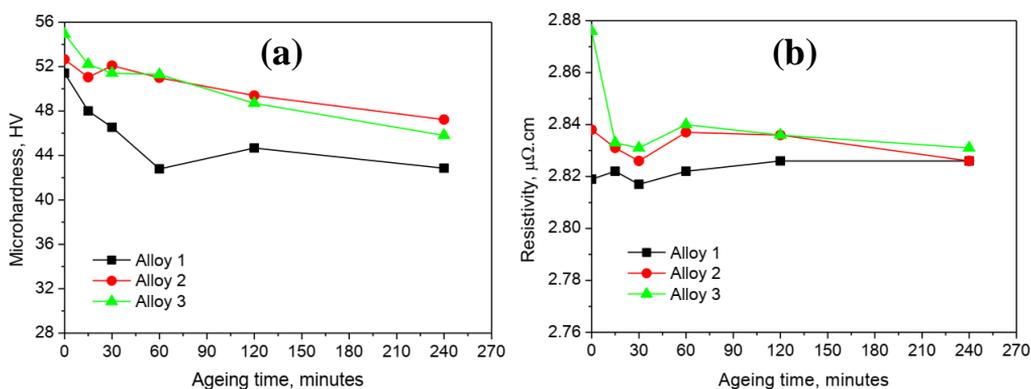

Fig. 3. Variation of (a) hardness and (b) electrical resistivity of 75% cold rolled alloys with isothermal ageing at 250°C

Tensile properties

The results of ultimate tensile strength and percentage elongation with their corresponding isochronal ageing conditions are graphically illustrated in Fig. 4. In case of tensile strength the double aging peaks are shown for trace impurities added alloys and achieve the higher strength (Fig. 4a).   It is due to formation of GP zones and metastable phases into the alloys. At the initial stage of aging, fine and profuse GP zones homogeneously distribute in the matrix which increases the strength of the alloys. After that these GP zones dissolve before formation of metastable phase as a result decreases in strength. On the other hand, metastable phases formed at the inter-mediate stage of aging and kept semi-coherence with the matrix are effectively resistant to the movement of dislocation so certain strengthening effect is observed [29, 30]. Beyond the ageing temperature at 250°C the sharp decreases of strength is due to precipitation coarsening and recrystallization of the alloys [31]. In case of the elongation of the experimental alloys small decreases up to around 150°C, then it turns to increase at higher temperature as shown in Fig. 4b. When the alloys are subjected to cold rolling, dislocation cell structures are formed by interacting with impurities. As well as dissolved silicon segregates or precipitates on the cell boundaries, causes the decreases of elongation. At a higher temperature, the precipitates are dissolved again. As a result, recovery and recrystallization occur. It is considered that stabilization of the subgrains is related to the segregation or precipitation of the dissolved impurities, iron and silicon [32, 33].
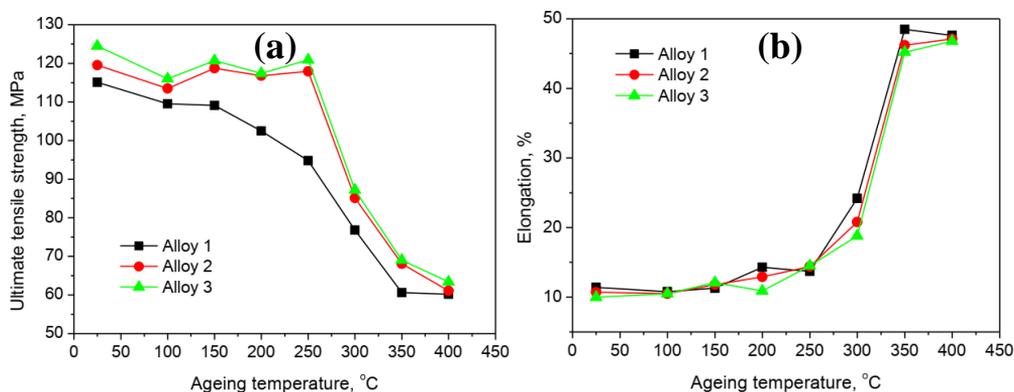

Fig. 4. Variation of (a) ultimate tensile strength and (b) percentages of elongation of 75% cold rolled alloys with ageing temperature for one hour and tensile tested at strain rate of $10^{-3}s^{-1}$

DSC study

Fig. 5 present DSC curves for all the alloys after 75% cold rolled state. From the DSC analysis all the figures content an endothermic peak at 145°C to 160°C. It is corresponded to dissolution of some phases already present into the alloys. Commercially pure Al Alloy 1 shows the insignificant peak due to negligible amount of impurities (Fig. 5a). In case of trace added Alloy 2 the small endothermic peak is observed as a small amount of impurities presents into the alloy (Fig. 5b) and Alloy 3 shows the broad endothermic peak for higher dissolution of phases in the alloy (Fig. 5c) [34, 35]. It is also observed that higher impurities takes the relatively higher temperature for disolution of some phases.
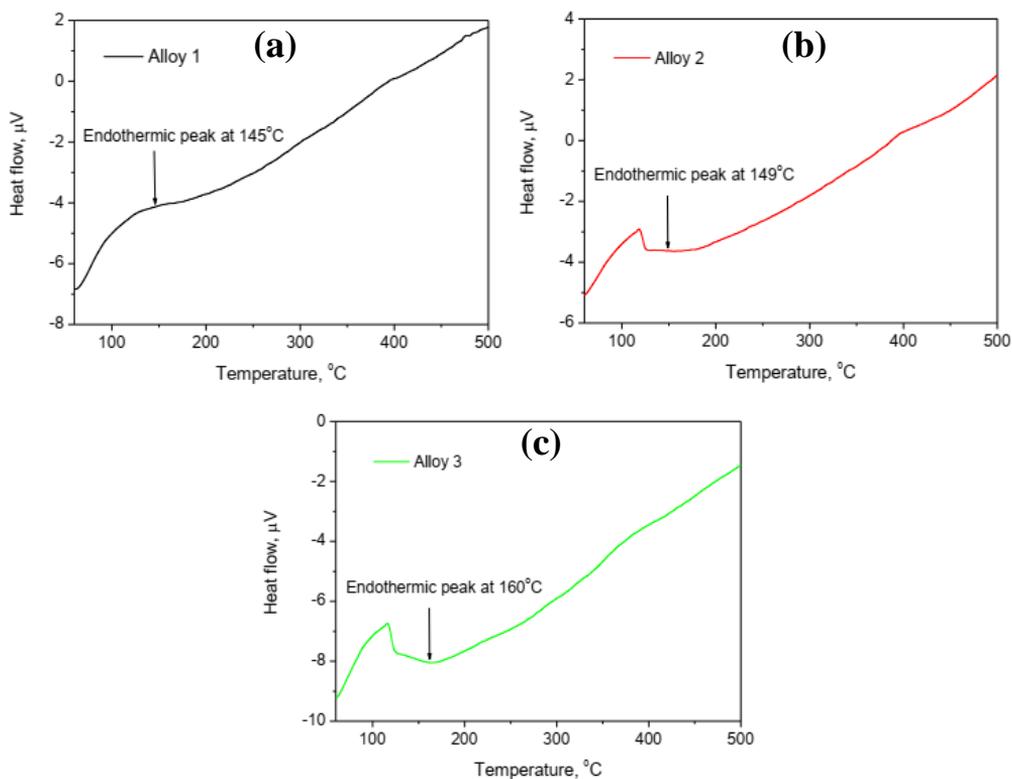
Fig. 5. DSC heating curve of a) Alloy 1, b) Alloy 2 and c) Alloy 3

Optical microscopy

Figure. 6a-c shows the optical micrograph of the commercially pure Alloy 1 and trace added Alloy 2 and Alloy 3 after application of 75% rolling reduction. These micrographs show typical strained structure. It may be confirmed that firmly elongated grains along the rolling direction are observed through the optical microscope. The size and density of the particles are a function of the contents of Fe and Si in the alloys. In Alloy 1 the particles are small and scattered on the matrix (Fig. 6a). With the increase of Fe and Si contents in Alloy 2, the density of the particles increased correspondingly (Fig. 6b). Further increasing of Fe and Si in Alloy 3 gave rise to a significant increase in the particles (Fig. 6c) [36]. If the alloys are aged at 400°C for 60 minutes, fully recrystallized structures are shown for each case (Fig. 6. d-f). At higher temperature of ageing, recrystallization took place. The most inhomogeneous microstructure is also found for the alloys. The elongated grains and rolling direction are almost absent in to the microstructure. The dendrites appear to be dissolved and the precipitates lie on grain boundaries while precipitation coarsening occurred. At the same time as fine equiaxed grains developed in to the microstructures [37, 38].
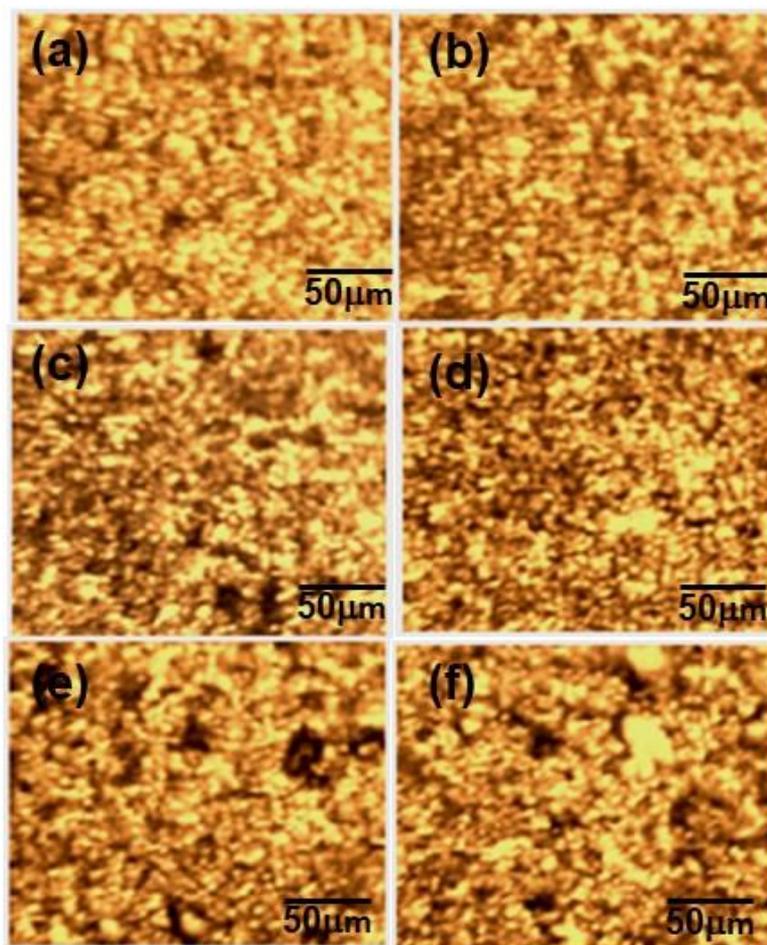
Fig. 6. Optical microscopy images of 75% cold rolled a) Alloy 1, b) Alloy 2 and c) Alloy 3 and after ageing at 400°C for one hour d) Alloy 1, e) Alloy 2 and f) Alloy 3

Scanning electron microscopy

Figure 7 shows the SEM images of as-rolled alloys with 75% rolling reduction at room temperature. The microstructures of all the alloys are mainly composed of a fine α-Al + Si eutectic mixture, eutectic silicon and other Fe rich intermetallic phases [39, 40]. Eutectic silicon and other Fe rich intermetallic phases are more visible in trace added alloys especially in Alloy 3. It contents the higher percentages of Si and Fe as shows in table 1. The consequent EDX of the experimental alloys for the chosen area of the SEM shown in Figs. 7a-c. The following elements of weight percentage are found in this area of Alloy 1, 92.75% Al, 5.37% Si, 0.17 % Cr, 0.15% Fe, 0.61% Ni, 0.42% Cu and 0.53% Zn, Alloy 2 are 87.53% Al, 11.43% Si, 0.67% Fe, 0.37% Cu and Alloy 3 are 77.81% Al, 18.20% Si, 1.38% Cr, 0.60% Mn, 1.14% Fe, 0.29% Cu and 0.30% Zn respectively. From the analysis Alloy 1 shows the minimum impurities than Alloy 2 and the volume fraction of the particles is the largest in Alloy 3.
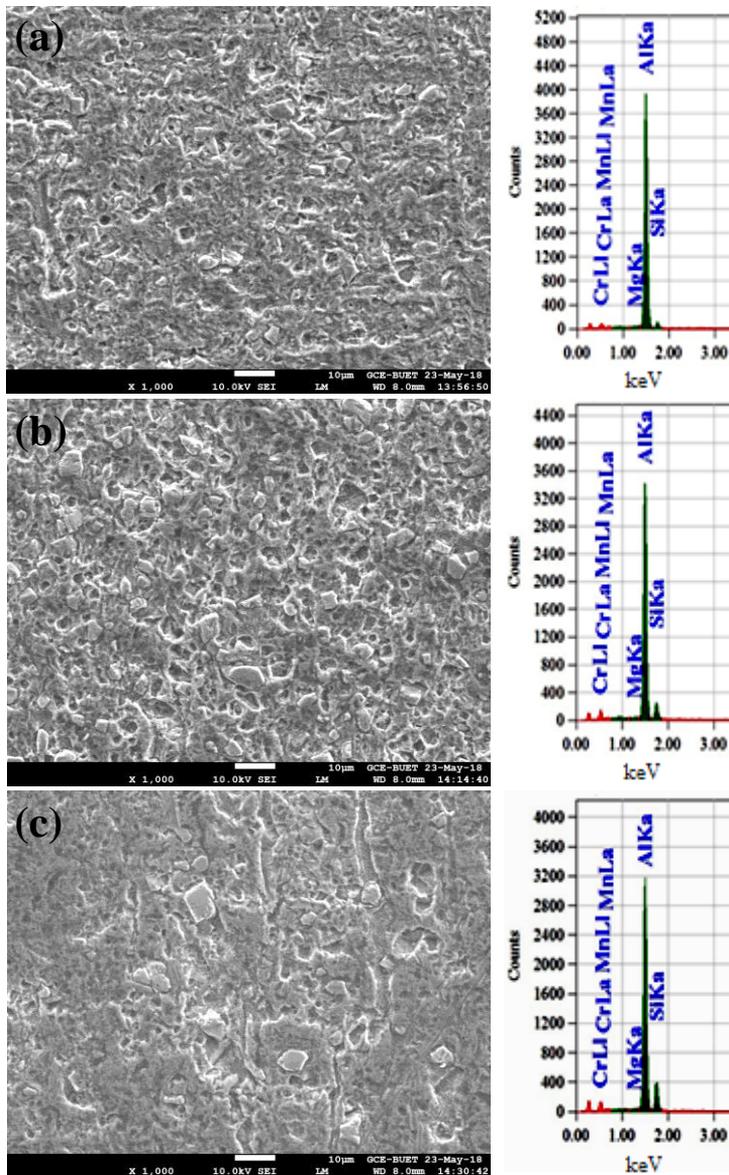
Fig. 7. SEM images and EDX analysis of 75% cold rolled a) Alloy 1, b) Alloy 2 and c) Alloy 3 aged at 200°C for one hour

Figure 8 shows the fracture surfaces from this investigation of commercially pure aluminium Alloy 1, the trace impurities added Alloy 2 and Alloy 3 tensile tested at $10^{-3}s^{-1}$. The SEM images of fracture surfaces show spherical "dimples" correspond to microvoids that initiate crack formation. The fracture surfaces display smooth and flat areas separated by bright ridges which indicates a typical characteristic of the ductile fracture. The flat areas are hacked silicon particles. Fracture crack propagation is along grain boundaries. The fracture of aluminum alloys is often initiated by the cracking of silicon particles as studied earlier. Generally pure metals are ductile in nature (Fig. 8a) [41, 42].
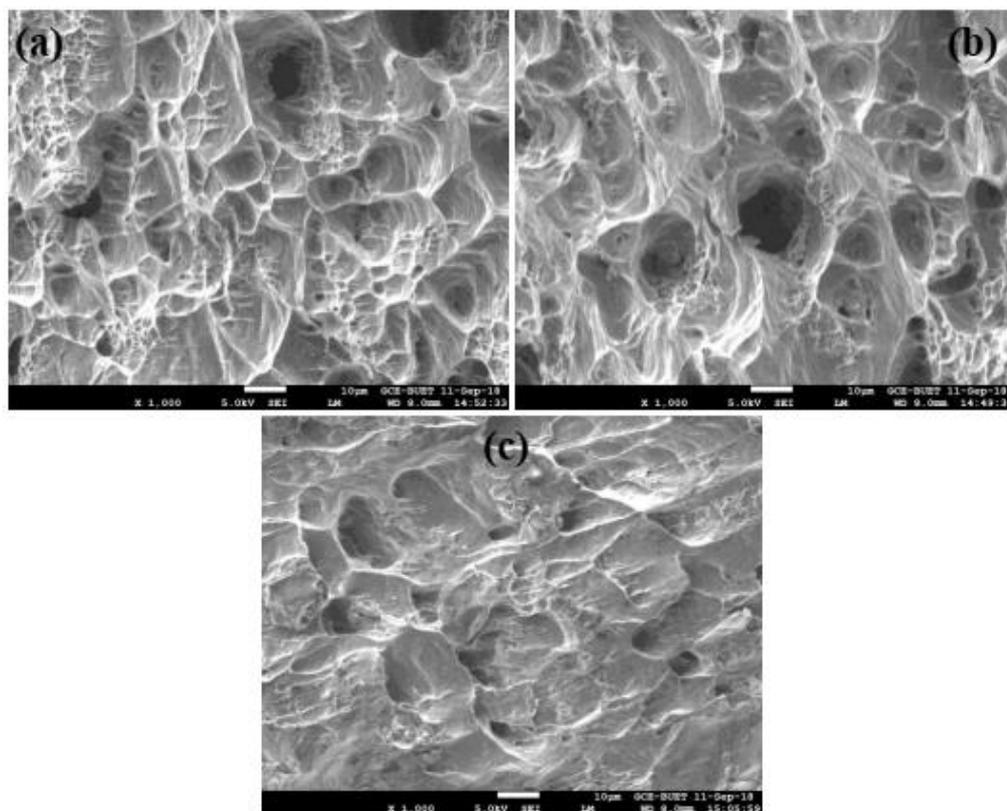
Fig. 8. SEM fractograph of 75% cold deformed a) Alloy 1, b) Alloy 2 and c) Alloy 3, aged at 200°C for 1 hour and

tensile tested at strain rate of $10^{-3}s^{-1}$

The addition of impurities to the metal makes the movement of dislocations within the metal difficult. This decreases the ability of the metal to sustain the plastic deformation. Thus the ductility decreases and brittleness increases. Higher amount of impurities into the alloys decrease the dimples and become shallower on the fracture surfaces (Fig. 8b, and 8c). As a result the ductility reduces as well as the grain size decreases [43].

Conclusions

Properties of the commercially pure aluminium after repeated melting are observed. The hardness of the alloys increases with the degree of deformation because of strain hardening effects. On the other hand, initially in a decrease in the electrical resistivity may possibly to pin hole or porosity reduction into the alloys and heavily cold working increases the resistivity of the alloys may be due to material defects like dislocations. The trace impurities improve the hardness of the commercially pure aluminium due to presence of different intermetallics of Fe, Si etc. During ageing the trace added alloys attain the higher strength due to formation of GP zones as well as metastable phase. As the impurities increase the ductility of the alloys decreases and brittleness increases. The dimples into the fracture surfaces also decrease frequently and become shallower with the increasing of impurities. These types of alloys recrystallized fully beyond ageing at 300°C for 60 minutes.

References

[1]   J. Hirsch, B. Skrotzki, G. Gottstein, *Aluminium Alloys: Their Physical and Mechanical Properties,* **Wiley, Weinheim, Germany,** 2008.

[2]   F.C. Campbell, *Elements of Metallurgy and Engineering Alloys,* **ASM International, Materials Park, Ohio,** 2008.

[3]   J.R. Davis, *Corrosion of Aluminum and Aluminum Alloys,* **ASM International, Materials Park, Ohio,** 1999.

[4]   M.S. Kaiser, *Effect of trace scandium addition on Al-6Mg alloy. Journal of Mechanical Engineering,* **Transaction of the Mech. Eng. Div, 36,** 2006, pp. 12-17.

[5]   F. Stadler, H. Antrekowitsch, W. Fragner, H. Kaufmann, P.J. Uggowitzer, *Effect of main alloying elements on strength of Al–Si foundry alloys at elevated temperatures,* **International Journal of Cast Metals Research, 25(4),** 2012, pp. 215-224.

[6]   H.T Naeem, K.S. Mohammed, K.R. Ahmad, A. Rahmat, *The influence of nickel and tin additives on the microstructural and mechanical properties of Al-Zn-Mg-Cu alloys,* **Advances in Materials Science and Engineering, 2014,** 2014, pp. 1-10.

[7]   M.S. Kaiser, S. Datta, A. Roychowdhury, M.K. Banerjee, *Effect of scandium on the microstructure and ageing behaviour of cast Al-6Mg alloy,* **Materials Characterization, 59(11),** 2008, pp. 1661-1666.

[8]   H.M. Medrano-Prieto, C.G. Garay-Reyes, C.D. Gomez-Esparza, J. Aguilar-Santillán, M.C. Maldonado-Orozco, R. Martínez-Sanchez, *Evolution of microstructure in Al-Si-Cu system modified with a transition element addition and its effect on hardness,* **Materials Research, 19(1),** 2016, pp. 59-66.

[9]   M.S. Kaiser, *Solution treatment effect on tensile, impact and fracture behaviour of trace Zr added Al-12Si-1Mg-1Cu piston Alloy,* **Journal of the Institution of Engineers, India, Series D. 99(1),** 2018, pp. 109-114.

[10] R.S. Rana, R. Purohit, S. Das, *Reviews on the influences of alloying elements on the microstructure and mechanical properties of aluminum alloys and aluminum alloy composites,* **International Journal of Scientific and Research Publications, 2(6),** 2012, pp. 1-7.

[11] G.T. Abdel-Jaber, A.M. Omran, K.A. Khalil, M. Fujii, M. Seki, A. Yoshida, *An Investigation into solidification and mechanical properties behavior of Al-Si casting alloys,* *I***nternational Journal of Mechanical and Mechatronics Engineering, 10(4),** 2010, pp. 30-35.

[12] S.G. Shabestari, H. Moemeni, *Effect of copper and solidification conditions on the microstructure and mechanical properties of Al-Si-Mg alloys,* **Journal of Materials Processing Technology, 153-154,** 2004, pp. 193-198.

[13] Z. Liuy, G. Zu, H. Luo, Y. Liu, G. Yao, *Influence of Mg addition on graphite particle distribution in the Aluminum alloy matrix composites,* **Materials Science Technology, 26(3),** 2010, pp. 244-250.

[14] S. Ren, X. He, X. Qu, I.S. Humail, Y. Li, *Effect of Mg and Si in the aluminum on the thermo-mechanicalproperties of pressureless infiltrated SiCp/Al composites,* **Science and Technology, 67,** 2007, pp. 2103-2113.

[15] C. Smith, *Grains, phases, and interfaces: As interpretation of microstructure,* **MET TECHNOL, 15(9),** 1948, pp. 1-37.

[16] M.S. Kaiser, *Effect of scandium on the softening behaviour of different degree of cold rolled Al-6Mg alloy annealed at different temperature,* **International Journal of Advances in Materials Science and Engineering. 1(1),** 2014, pp. 39-49.

[17] H. Yoshida, Y. Ookubo, *Effect of precipitation of impurities during annealing on the rate of recovery and recrystallization in 1050 aluminum hot-rolled sheets,* **Materials Transactions, 56(12),** 2015, pp. 1960-1967.

[18] M.S. Kaiser, *Precipitation and softening behaviour of cast, cold rolled and hot rolling prior to cold rolled Al-6Mg alloy annealed at high temperature,* **Journal of Mechanical Engineering, Transaction of the Mech. Eng. Div., 45(1),** 2015, pp. 32-36.

[19] C.S. Çetinarslan, *Effect of cold plastic deformation on electrical conductivity of various materials,* **Materials and Design, 30(3),** 2009, pp. 671-673.

[20] S.O. Adeosun, O.I. Sekunowo, S.A. Balogun, L.O. Osoba, *Effect of deformation on the mechanical and electrical properties of aluminum-magnesium alloy,* **Journal of Minerals and Materials Characterization and Engineering, 10(6),** 2011, pp. 553-560.

[21] S. Nestorovi, *Influence of deformation degree at cold-rolling on the anneal hardening effect in sintered copper-based alloy,* **Journal of Mining and Metallurgy, 40B(1),** 2004, pp. 101-109.

[22] A. Manuel, S. Guapuriche, Y.Y. Zhao, *A. Pitman, A. Greene, Correlation of strength with hardness and electrical conductivity for aluminium alloy 7010,* **Materials Science Forum, 519-521,** 2006, pp. 853-858.

[23] M.S. Kaiser, S. Datta, A. Roychowdhury, M.K. Banerjee, *Age hardening behaviour of wrought Al-Mg-Sc alloy,* **Journal of Materials and Manufacturing Processes. 23(1),** 2008, pp. 74-81.

[24] R.X. Li, R.D. Li, Y.H. Zhao, L.Z. He, C.X. Li, H.R. Guan, Z.Q. Hu, *Age-hardening behavior of cast Al–Si base alloy,* **Materials Letters. 58(15),** 2004, pp. 2096-2101.

[25] J.D. Bryant, *The effects of preaging treatments on aging kinetics and mechanical properties in AA6111 aluminum autobody sheet,* **Metallurgical and Materials Transactions A. 30(8),** 1999, pp. 1999-2006.

[26] K. Matsuda, H. Gamada, K. Fujil, Y. Uetani, T. Sato, A. Kamio, S. Ikeno, *High-resolution electron microscopy on the structure of Guinier–Preston zones in an Al-1.6 mass pct Mg2Si alloy,* **Metallurgical and Materials Transactions, 29A,** 1998, pp. 1161-1167.

[27] C. Li-xin, L. Zhen-xing, Z. Xiao-guang, T. Jian-guo, L. Ke, L. Xing-xing, Q. Chen, *Precipitation of metastable phases and its effect on electrical resistivity of Al-0.96Mg2Si alloy during aging,* **Transactions of Nonferrous Metals Society of China, 24(7),** 2014, pp. 2266-2274.

[28] P. Mukhopadhyay, *Alloy designation, processing, and use of AA6XXX series aluminium alloys,* **International Scholarly Research Network, 2012,** 2012, pp. 1- 15.

[29] M.S. Kaiser, *Efffect of solution treatment on the age hardening behaviour of Al-12Si-1Mg-1Cu piston alloy with trace Zr addition,* **Journal of Casting and Materials Engineering, 2(2),** 2018, pp. 30-37.

[30] S. Shivkumar, C. Keller, D. Apelian, *Aging behavior in cast Al-Si-Mg alloys,* **AFS Transactions, 98,** 1990, pp. 905-911.

[31] H. Yoshida, Y. Ookubo, *Effect of precipitation of impurities during annealing on the rate of recovery and recrystallization in 1050 Aluminum hot-rolled sheets,* **Journal of Japan Institute of Light Metals, 64(7),** 2014, pp. 285-291.

[32] W. Jinlian, X. Jun, P. Feng, *Effect of annealing on microstructure and properties of Er modified 5052 alloy,* **Results in Physics, 10,** 2018, pp. 476-480.

[33] W. Bo, C. Xian-hua, P. Fu-sheng, M. Jian-jun, F. Yong, *Effects of cold rolling and heat treatment on microstructure and mechanical properties of AA 5052 aluminum alloy,* **Trans. Nonferrous Met. Soc. China, 25,** 2015, pp. 2481-2489.

[34] F. Lasagni, A. Falahati, H.M. Semnani, H.P. Degischer, *Precipitation of Si revealed by dilatometry in Al-Si-Cu/Mg alloys,* **Kovove Mater. 46,** 2008, pp. 1-6.

[35] M.S. Kaiser, *Thermal analysis and kinetics of the precipitation in wrought Al-Mg, Al-Mg-Sc and Al-Mg-Sc-Me (Me=Zr, Ti) alloys,* **Iranian Journal of Materials Sciences and Engineering, 10(3),** 2013, pp. 19-29.

[36] J. Dong, Q. Dong, Y. Dai, H. Xing, Y. Han, J. Ma, J. Zhang, J. Wang, B. Sun, *Microstructure evolution in high purity aluminum single crystal processed by equal channel angular pressing (ECAP),* **Materials, 10(87),** 2017, pp. 1-8.

[37] L. Zhang, Y. Wang, X. Yang, K. Li, S. Ni, Y. Du, M. Song, *Texture, microstructure and mechanical properties of 6111 aluminum alloy subject to rolling deformation,* **Materials Research. 20(5),** 2017, pp. 1360-1368.

[38] L. Radovic, M. Nikacevic, *Microstructure and properties of cold rolled and annealed Al-Mg alloys,* **Scientific Technical Review, 8(2),** 2008, pp. 14-20.

[39] O.H. Yakubu, I. Usman, A. Aliyu, O.O. Emmanuel, *Influence of iron content and plastic deformation on the mechanical properties of 8011-type Al-Fe-Si alloy,* **Nigerian Journal of Technology. 35(1),** 2016, pp. 122-128.

[40] Y. Liu, Y. Sun, L. Zhang, Y. Zhao, J. Wang, C. Liu, *Microstructure and mechanical properties of Al-5Mg-0.8Mn alloys with various contents of Fe and Si cast under near-rapid cooling,* **Metals, 7(10),** 2017, pp. 1-12.

[41] L.H. Ha, L. Li, J. Sun, *Ductile to brittle transition of pure Al sheet constrained by strength mismatched parallel bi-interface,* **Scripta Materialia, 52(11),** 2005, pp. 1157-1162.

[42] H. Mae, X. Teng, Y. Bai, T. Wierzbicki, *Comparison of ductile fracture properties of aluminum castings: Sand mold vs. metal mold,* **International Journal of Solids and Structures, 45,** 2008, pp. 1430-1444.

[43] G.D. Motsi, M.B. Shongwe, T.J. Sono, P.A. Olubambi, *Anisotropic behavior studies of aluminum alloy 5083-H0 using a micro-tensile test stage in a FEG-SEM,* **Materials Science and Engineering, 656,** 2016, pp. 266-274.